

where N_v is Avogadro's number, V_m the molar volume of BaTi_4O_9 , f the mole fraction of Ba ions in BaTi_4O_9 , and $f=1/14$. In this analysis, it is implicitly assumed that Ti from the TiO_2 substrate and oxygen from the ambient are readily available and they react with Ba to form the needles of a BaTi_4O_9 phase. We further assume that both the reaction kinetics and the oxygen and titanium transports are not the rate-limiting steps in the needle growth.

From Eqs. (2) and (3), we obtain

$$\delta D_s \frac{\Delta c}{c} = b d \frac{dx N_v}{dt V_m} \quad (4)$$

Integration of Eq. (4) gives

$$x^2 = \frac{2 D_s \delta \Delta c V_m t}{b f N_v} \quad (5)$$

or

$$D_s \delta = \frac{x^2 b f N_v}{2 t \Delta c V_m} \quad (6)$$

The needle-growth kinetics given in Fig. 4 do not fit a parabolic time dependence, as predicted by Eq. (5). However, the average

growth rate gives a rough estimate of Ba surface diffusivity. For $b=2 \mu\text{m}$ and $\Delta c \approx 5 \times 10^{18}$ Ba ions/ cm^3 , we obtain $\delta D_s = 3.2 \times 10^{-10} \text{cm}^2/\text{s}$ at 1070°C . If δ , the interface width through which the diffusion occurs, is $\leq 10^{-4} \text{cm}$, then $d_s > 3.2 \times 10^{-6} \text{cm}^2/\text{s}$ for Ba migration at 1070°C .

Acknowledgments: The authors thank M. Levinson for helpful discussions and the rutile crystal and J. Thomson for sample preparation.

References

- 1 H. M. O'Bryan, Jr. and J. Thomson, Jr., "Phase Equilibria in the TiO_2 -Rich Region of the System BaO-TiO_2 ," *J. Am. Ceram. Soc.*, **57** [12] 522-26 (1974).
- 2 P. Gordon and R. A. Vandermeer, "Grain-Boundary Migration"; pp. 205-66 in *Recrystallization Grain Growth and Textures*. American Society for Metals, Metals Park, OH, 1966.
- 3 M. H. Manghnani, E. S. Fisher, and W. S. Bower, Jr., "Temperature Dependence of the Elastic Constants of Single-Crystal Rutile Between 4 and 583°K ," *J. Phys. Chem. Solids*, **33** [11] 2149-59 (1972).
- 4 M. F. Yan and W. W. Rhodes, "Effects of Cation Contaminants in Conductive TiO_2 Ceramics"; to be published in *Journal of Applied Physics*.
- 5 J. P. Wittke, "Diffusion of Transition Metal Ions into Rutile (TiO_2)," *Electrochem. Soc.*, **113** [2] 193-94 (1966).
- 6 T. S. Lundy and W. A. Coghlan, "Cation Self Diffusion in Rutile," *J. Phys. (Paris) Colloq.*, **34** [9] 299-302 (1973).
- 7 D. A. Venkatu and L. E. Poteat, "Diffusion of Titanium in Single Crystal Rutile," *Mater. Sci. Eng.*, **5** [5] 258-62 (1969/70).
- 8 R. Haul and G. Dümbgen, "Self-diffusion of Oxygen in Rutile Crystals," *J. Phys. Chem. Solids*, **26** [1] 1-10 (1965).

Microstructure Development of Aluminum Oxide: Graphite Mixture During Carbothermic Reduction

F. J. KLUG,* W. D. PASCO,* and M. P. BOROM*

Ceramics Branch, Physical Chemistry Laboratory, General Electric Company,
Corporate Research and Development, Schenectady, New York 12301

Reactions in the system Al-O-C are discussed. Reaction conditions which produce an α -alumina body having a <70%-dense bulk region coated with an impervious, $\approx 100\text{-}\mu\text{m}$ thick surface layer are described. The development of the unique composite microstructure is attributed to reactions which serve to coarsen internal grains by vapor-phase transport of volatile aluminum suboxides and, thereby, reduce firing shrinkage. Proper control of the furnace atmosphere is necessary to produce the thin, dense surface layer. The effect of varying the carbon/alumina molar ratio on linear firing shrinkage, fired density, and weight loss was examined. In addition, the effect of oxygen partial pressure on the oxidation of carbon and the formation of an intermediate reaction product, $\text{Al}_4\text{O}_4\text{C}$, was examined.

I. Introduction

DIRECTIONALLY solidified nickel-based eutectic superalloys, such as NiTaC, have been identified as having mechanical properties superior to those of equiaxed or conventionally solidified superalloys.¹ However, until the present work was performed, hollow airfoil shapes (i.e. air-cooled vanes and blades for aircraft gas turbines) containing geometrically complex cooling passages could not be fabricated from NiTaC alloys because of a lack of suitable core materials.

The only practical method for forming geometrically complex cooling passageways is by casting the alloy around a leachable, ceramic core which has been fabricated by injection or transfer molding. The fabrication of a hollow airfoil shape is accomplished by the investment casting process. In this process, a wax pattern in the shape of the turbine blade is injected around the ceramic core

and an investment shell mold is subsequently fabricated around the wax pattern. The wax pattern is removed from the mold either by steam or by heating. The mold-core assembly is then fired to develop the properties required for the metal casting operation. After casting, the ceramic core is leached from the blade to open the internal cooling passageways.

The investment casting process requires that the core be: (1) chemically compatible with the molten alloy, which may contain 10 or more elements; (2) easily removable after casting by chemically benign means (mechanical removal is often impractical because of complex shapes); (3) crushable, so that triaxial compressive stresses in the core arising from the thermal expansion mismatch during cooling do not crack the alloy via associated tensile hoop stresses; (4) resistant to penetration by the molten alloy through reduction in open porosity at the core surface; and (5) dimensionally stable (metal wall thicknesses on the order of $0.076 \pm 0.007 \text{cm}$ establish tight tolerances on geometrical distortion of the core during fabrication and subsequent casting).

Silica-based core materials are used to cast superalloys at $T < 1550^\circ\text{C}$; they cannot be used with nickel-based eutectic superalloys such as NiTaC, however, since casting temperatures exceed 1700°C and molten-metal/ceramic contact times approach 20 h. A search for ceramic core materials which are chemically compatible with NiTaC alloys was reported by Huseby and Klug,² who used sessile drop tests to screen numerous compounds at $T = 1700^\circ$ to 1800°C . The results indicated that yttrium aluminate, lanthanum aluminate, alumina, and alumina-rich spinel were all chemically acceptable candidates.

Another major selection criterion, leachability, is also dependent on the chemical properties of the core material. Arendt *et al.*³ demonstrated that molten salts, such as Li_3AlF_6 , can be used to leach the above compounds. However, the process was technologically difficult and chemical attack of the alloy often occurred.⁴ Borom⁵ observed that low-density, high-purity alumina could be removed from castings using high-temperature aqueous

Presented at the Basic Science and Nuclear Divisions Fall Meeting, The American Ceramic Society, Hyannis, Massachusetts, September 27, 1977 (Paper No. 46-BN-77F). Received July 16, 1981; revised copy received February 8, 1982; approved June 8, 1982.

Supported by the Air Force Materials Laboratory under Contract No. F33615-76-C-5110.

*Member, the American Ceramic Society.

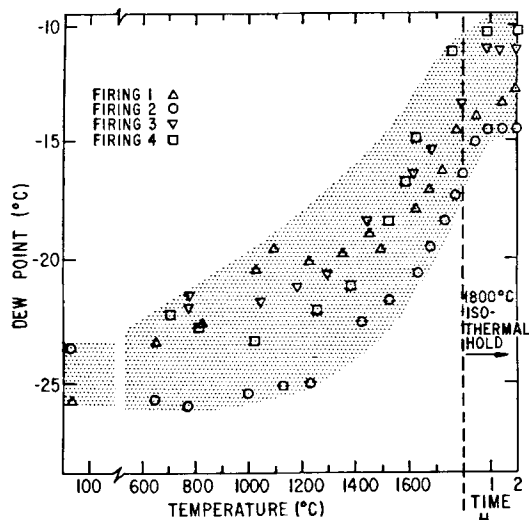


Fig. 1. Graph of dew point vs temperature for the "wet" H_2 furnace used in firing graphite/alumina samples at a heating rate of $300^\circ\text{C}/\text{h}$. Also shown is variation of dew point with time during 1800°C isothermal hold.

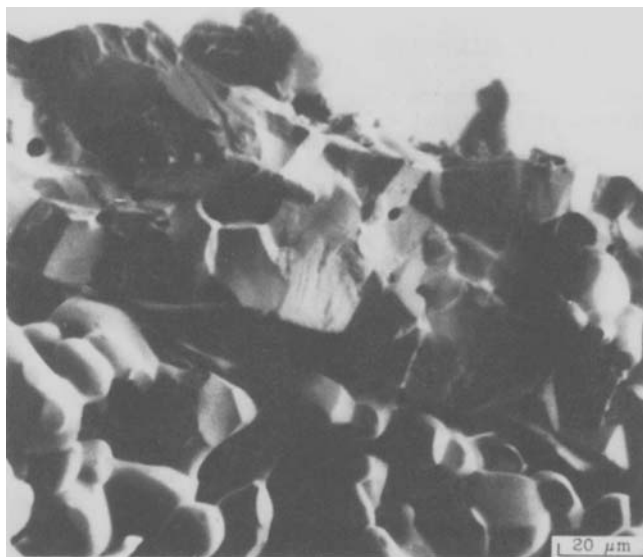


Fig. 2. Scanning electron micrograph of specimen containing a graphite/alumina molar ratio of 0.75 fired to 1750°C for 1 h in "wet" H_2 . Micrograph illustrates the bulk porosity of 60% enclosed by a dense alumina skin.

caustic solutions at rates comparable to the commercial removal of silica cores.

Alumina, therefore, has the requisite chemical properties for successful use as an advanced core material. However, it was still necessary to develop a crushable, structurally sound, dimensionally stable, molten-metal-impervious alumina core—properties which are each influenced by fabrication parameters. The current work achieves the property goals by utilizing the chemical reactions in the system Al-O-C-H to produce an aluminum oxide core material with a unique microstructure characterized by a highly porous interior surrounded by a high-density surface layer. The microstructure development is a consequence of a chemical reaction between alumina and graphite, which produces volatile aluminum suboxides and carbon monoxide. The removal of graphite and

some alumina subsequently increases porosity and crushability. Proper control of the hydrogen gas dew point during the alumina/graphite reaction results in creation of a dense skin of alumina surrounding the highly porous and crushable interior. The dense layer serves to prevent metal penetration, whereas the porous interior enhances crushability, thus preventing hot cracking of the alloy.

II. Experimental Procedure

(1) Furnace Construction

"Wet" H_2 firings were conducted in large, Mo-wire-wound tube furnaces insulated with porous alumina bricks and contained in a metal shell. One end of the tube was open to the atmosphere. There was no provision for sealing against air infiltration except for the positive pressure in the furnace due to hydrogen flow. Outgassing of the refractories and air infiltration into the Mo-wound tube furnace during thermal cycling resulted in large but fairly reproducible changes in the oxygen partial pressure during each sintering run. The P_{O_2} of the furnace was measured as a function of temperature by pumping gas out of the hot zone through an alumina tube into a zirconia oxygen sensor.

"Dry" H_2 firings (-37°C dew point) were conducted in a small laboratory BHO furnace⁶ which used a molybdenum-foil resistance heater. Thermal insulation was provided by Mo radiation shielding contained within a fused silica tube (13 cm OD). Water-cooled copper end plates were sealed to the fused silica tube with silicone rubber cement. The furnace was closed with O-ring-sealed, threaded end caps and H_2 was piped in and out through copper tubing. Experimental results indicated little or no leakage of air into the BHO.

A zirconia oxygen sensor* was used to monitor the dew point of both the inlet and the exit gas to determine the actual oxygen partial pressure in each of the furnaces.

(2) Sample Fabrication

Various mixtures of graphite[†] and alumina[‡] plus 47 to 49 vol% wax binder were prepared, giving graphite/alumina (G/A) molar ratios of zero to 1.25. The constituents were heated to 100° to 110°C , mixed in a sigma mixer, cooled, and granulated.

Samples used in trials reported in Fig. 2 and Figs. 6 through 9 were fabricated by cold-pressing the granulated mixture at 345 MPa. All other samples were formed by injection-molding the granulated mixture into small cylinders (0.93 cm in diam. by 1.3 cm high) at 2.8 MPa with a dwell time of 20 s.

(3) Binder Removal

Wax was removed from specimens for use in the "wet" H_2 studies by packing the samples in commercial alumina,[‡] heating at $\approx 50^\circ\text{C}/\text{h}$ to a presintering temperature, and holding at temperature for 1 h. Flowing H_2 (≈ 2000 L/h) was passed through a 20-L furnace. A presintering temperature of 1350°C was selected for the cold-pressed specimen of Fig. 2 to provide handling strength prior to final sintering. The presintering temperature for the injection-molded specimens of Figs. 3 to 5 was decreased to 1100°C to permit carbon burnout studies at $T = 1100^\circ$ to 1350°C . After the 1-h isothermal hold, specimens were removed from the hot furnace and cooled under flowing H_2 . Occasional specimen bloating occurred during the $50^\circ\text{C}/\text{h}$ presintering cycle. The bloated specimens were discarded.

In the "dry" H_2 studies with cold-pressed specimens (Figs. 6 to 9) it was recognized that specimen bloating could be reduced by decreasing the heating rate during dewaxing to $\approx 25^\circ\text{C}/\text{h}$ and that heating in air to 250°C in commercial alumina was sufficient to remove 98% of the binder with negligible loss of graphite. The residual binder provided enough strength to permit transfer of the specimens to the "dry" H_2 sintering furnace. Corrections were made for the residual binder in weight loss experiments.

In the final "dry" H_2 experiments (Fig. 10), which used

*AMETEK, Thermox Instruments Div., Ametek Inc., Pittsburgh, PA.

†325-mesh graphite, nominal purity 96.096; J. T. Baker Co., Phillipsburg, NJ.

‡38-900 alundum, average particle size $6\ \mu\text{m}$, 99.9% pure; Norton Co., Worcester, MA.

injection-molded specimens, dewaxing was performed using commercial carbon⁸ as the packing powder. Carbon was more easily removed from the specimen surfaces than alumina. Prior to the controlled atmosphere experiments of Fig. 10, and after dewaxing, samples were fired at $\approx 25^\circ\text{C}/\text{h}$ to 1100°C in "dry" H_2 .

(4) Firing Procedures

(A) "Wet" Hydrogen Furnace: Weight loss from dewaxed, injection-molded specimens as a function of firing time was studied in the "wet" H_2 furnace by removing samples at 15-min intervals from isothermal holds at $T = 1330^\circ, 1450^\circ, 1550^\circ, 1650^\circ,$ and 1750°C . Measurement of the isothermal hold time began the instant the sample reached temperature after a 5- to 6-min upquench from 25°C . After firing, the samples were air-quenched to room temperature, weighed, and measured. The air quench resulted in a small oxidative loss of carbon. Temperature was measured in the "wet" H_2 furnace using an optical pyrometer.

(B) "Dry" Hydrogen BHO Furnace: Specimens were placed in the BHO, which was purged with N_2 prior to introduction of a controlled-dew-point, hydrogen atmosphere in which the dew point was varied from a "dry" -37° (175 ppm H_2O) to 0°C (6062 ppm H_2O). The inlet gas to the furnace was continuously monitored for P_{O_2} via a zirconia oxygen sensor. The flow rate of the inlet gas was 108 L/h with a total furnace volume of 5.7 L. A $1300^\circ\text{C}/\text{h}$ heating rate was used, with a 30-min isothermal hold at maximum temperature. Samples were quenched from T_{max} at a rate of $200^\circ\text{C}/\text{min}$ in H_2 . Temperature measurements were performed using an optical pyrometer.¹

(5) Sample Characterization

All specimens were weighed and measured dimensionally before and after dewaxing and after firing to yield values of weight loss, corrected for loss of residual binder, and firing shrinkage. The ceramic ($\text{Al}_2\text{O}_3 + \text{C}$) weight loss was determined by subtracting the weight of the final specimen from the known weight of the ceramic in the original specimen. Density measurements were ascertained via Archimedes' principle. The microstructure of the specimens after sintering was examined via optical and scanning electron microscopy. Crystalline phases were identified by the Debye-Scherrer X-ray diffraction technique.

III. Results and Discussion

Carbon can be lost from the alumina compacts during firing, either by the reduction of alumina by carbon to form CO and volatile suboxides or, alternatively, by the oxidation of C by H_2O vapor in the hydrogen firing atmosphere. The relative importance of these two reaction paths on the development of microstructure is examined in the subsequent sections on "wet" and "dry" H_2 firings.

(1) "Wet" Hydrogen Firings

(A) Formation of a Dense Al_2O_3 Skin: Figure 1 illustrates the variation of dew point vs temperature for the Mo-wound tube furnace, as measured over four firing cycles. It is clear from the figure that the furnace atmosphere becomes more oxidizing as the temperature is increased during "wet" hydrogen firings. The most striking and impressive result of the experiments in "wet" H_2 is found in the final microstructures. An SEM photomicrograph of a fracture surface of a specimen with a G/A of 0.75 (Fig. 2) reveals the existence of a dense layer at the surface. X-ray diffraction verified that the dense skin was α -alumina. The microstructure is characterized by a dense continuous surface layer and a porous interior consisting of particles with a smooth, rounded morphology interconnected by narrow necks. Narrow neck connections have been demonstrated to enhance both leachability^{4,5} and crushability⁷ of such specimens. Firings conducted in "dry" H_2 in the BHO furnace exhibited no dense Al_2O_3 surface layer, indicating that formation of the layer can be regulated by controlling the oxygen

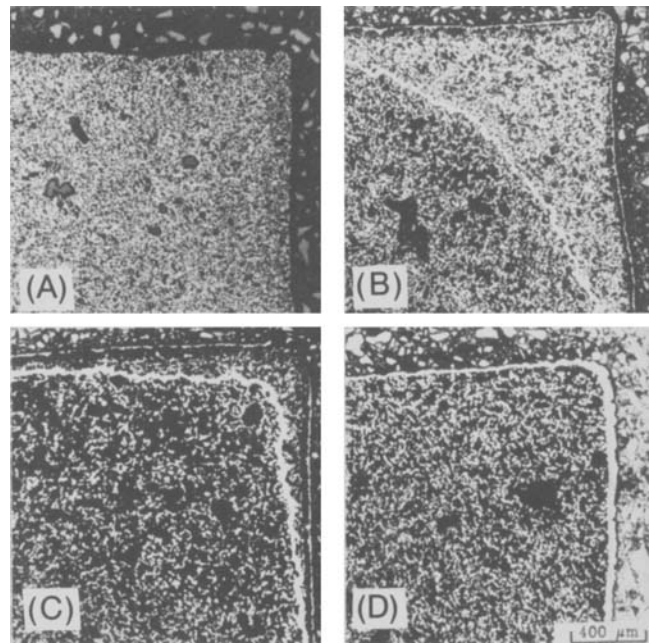


Fig. 3. Photomicrographs of cross sections of injection-molded specimen fired at 1750°C for 1 h in "wet" H_2 containing G/A molar ratios of (A) 0, (B) 0.25, (C) 0.375, and (D) 0.50, showing variation in microstructure, particularly in bulk density and in absence or location of dense alumina layer.

partial pressure, P_{O_2} , in the furnace atmosphere. The need for P_{O_2} control is illustrated in the microstructures shown in Fig. 3, which reveal that the dense continuous layer does not necessarily form at the surface of the specimen. As the G/A ratio decreases, for a given set of furnace conditions, the dense layer forms nearer the center of the specimen, with the most pronounced effect observed at the corners. In samples where a dense layer has formed within the bulk and sometimes also at the surface (see Fig. 3(B)), it is further noted that the density of the sample is lower inside the inner layer than outside. Such a structure is associated with a loss of density-controlling carbon in the peripheral regions due to atmospheric oxidation.

(B) Weight Loss of Alumina/Graphite Mixtures in "Wet" Hydrogen: To minimize the effect of atmospheric oxidation of carbon and to enable a more accurate measurement of the weight loss associated with the direct reaction between Al_2O_3 and C, specimens were plunged directly into a hot furnace (1330° to 1760°C). The weight loss of alumina plus carbon from samples during firing in "wet" hydrogen is plotted as a function of time at different temperatures in Fig. 4. At $T \leq 1450^\circ\text{C}$, the weight loss from the cylindrical samples appears to be linear with respect to time. Above 1550°C the reaction mode changes and the samples exhibit an initially rapid weight loss, which increases with temperature but diminishes with increasing time.

Inspection of metallographic cross sections of samples from the isothermal holds of 1330° through 1550°C shows a white outer ring, devoid of graphite and increasing in thickness with time, surrounding a darker core which contains graphite. The growth of the white volume also bears a linear relation with time, supporting the contention that the lower-temperature weight loss is due to atmospheric oxidation of carbon. Samples taken at 1650°C , however, exhibited both a new phase and a macrostructure different from those observed at lower temperatures.

The new phase in the 1650°C samples was found to be $\text{Al}_4\text{O}_4\text{C}$. Examination of the cross sections shown in Fig. 5 reveals that macroscopic spheres containing $\text{Al}_4\text{O}_4\text{C}$ exist in a narrow ring which moves progressively toward the center of the sample with increasing time at 1650°C and eventually disappears. In addition to the $\text{Al}_4\text{O}_4\text{C}$ band, two additional bands can be identified in Fig. 5(B), one inside and one outside the $\text{Al}_4\text{O}_4\text{C}$ band. The outer

⁸Vulcan XC-72, Cabot Corp., Boston, MA.

¹Leeds and Northrup, North Wales, PA.

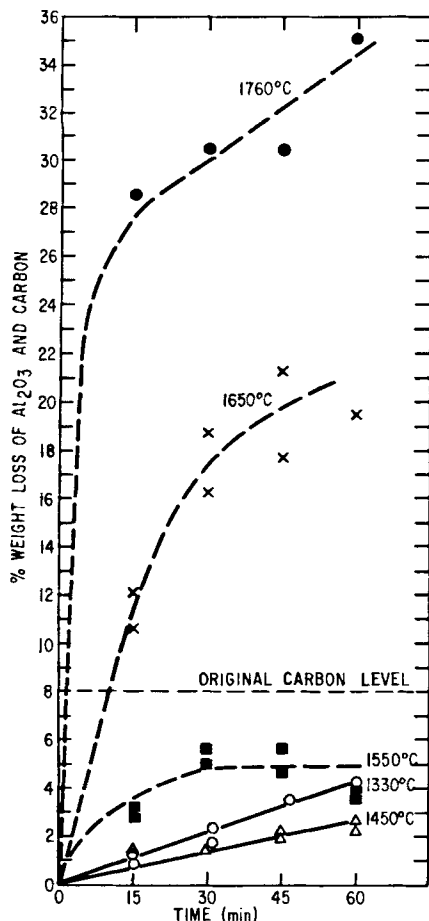


Fig. 4. Plot of percent weight loss vs firing time for injection-molded samples with a G/A molar ratio of 0.75; firings were conducted in "wet" H_2 .

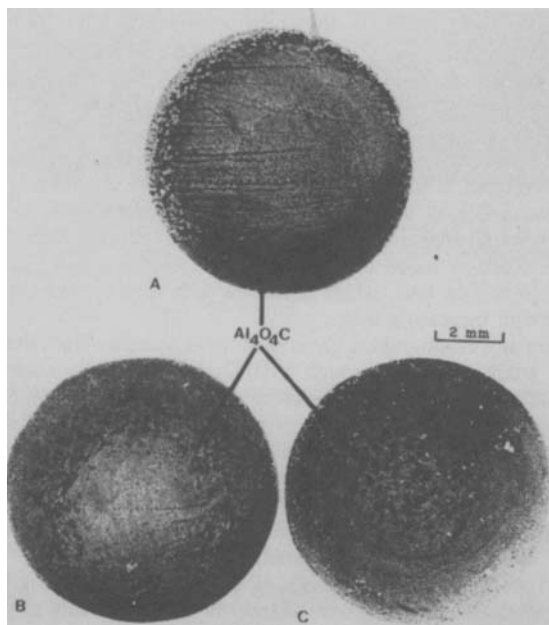


Fig. 5. Macrographs of cross sections injection-molded graphite/alumina cylindrical specimens with G/A=0.75 fired in "wet" H_2 at 1650°C for (A) 15 min, (B) 30 min, and (C) 45 min, showing the presence of a zone of Al_4O_4C which moves toward the center of the specimen with time.

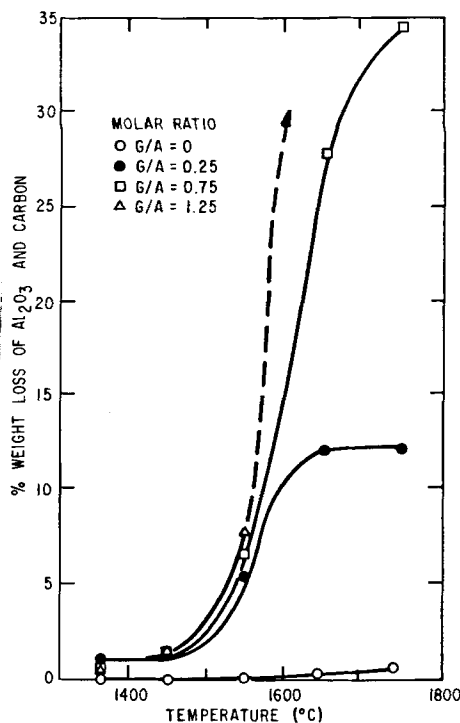


Fig. 6. Plot of percent total weight loss vs temperature for compacts having G/A molar ratios of 0.0, 0.25, 0.75, and 1.25 and fired in "dry" H_2 for 30 min.

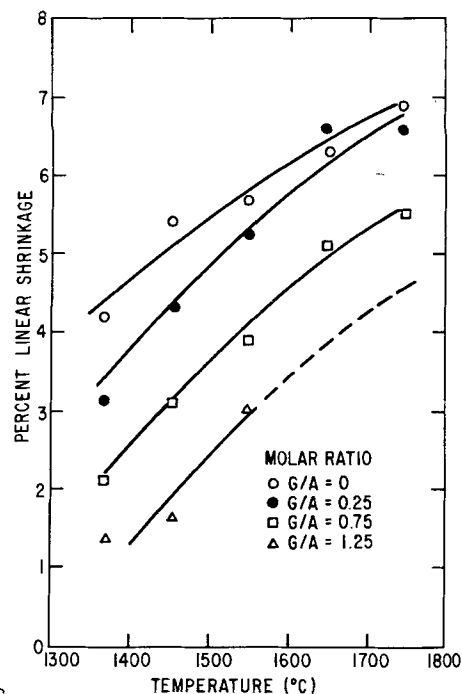


Fig. 7. Plot of percent linear shrinkage vs temperature for cold-pressed compacts having G/A molar ratios of 0, 0.25, 0.75, and 1.25 and fired in "dry" H_2 for 30 min.

band is a porous microstructure devoid of graphite; the inner band, however, contains an unreacted graphite/alumina mixture. The formation of the intermediate compound (Al_4O_4C) during the reduction of alumina is addressed in more detail in Section III (2)(A).

The preceding experiments showed that the partial pressure of oxygen affects both the sintering behavior and skin formation in graphite-alumina compacts. However, the exact oxygen partial pressure needed to produce a porous body, while simultaneously producing a dense continuous skin, was not defined. It was expected that no skin formation would occur at low P_{O_2} and that a porous crushable body would result. In contrast, a higher-density compact was expected to result from high P_{O_2} levels due to atmospheric oxidation of carbon from the compact before reduction of the Al_2O_3 could occur. Proper control of the P_{O_2} is clearly necessary to produce the desired microstructure. The following controlled-atmosphere firings were designed to delineate the required regions of P_{O_2} control.

(2) Firings in "Dry" H_2 (Dew Point $-37^\circ C$)

(A) *Identification of Overall Reaction:* A series of experiments was performed in flowing H_2 with a dew point of $-37^\circ C$, to minimize atmospheric oxidation of graphite prior to initiation of direct reaction between graphite and alumina. A rapid heating rate ($\approx 1300^\circ C/h$) was used to reach direct alumina/graphite reaction temperatures. The percent weight loss, percent linear shrinkage, and percent theoretical density attained are plotted, respectively, in Figs. 6, 7, and 8 as a function of the 30-min isothermal hold temperatures.

It can be seen from the weight loss data in Fig. 6 that a strong reaction involving a volatile species begins around 1500°C and accelerates with increasing temperature. The extent of the reaction increases with increasing G/A ratios. Weight loss data above 1550°C for G/A=1.25 are missing due to the highly fragile nature of the fired specimens. The small ($\approx 1\%$) weight loss observed for the graphite-free specimen is probably due to volatilization of alumina in the presence of flowing H_2 . Linear shrinkage, as illustrated in Fig. 7, increases with increasing firing temperature for each level of graphite addition, but the degree of shrinkage is

suppressed by increasing the ratio of G/A.

The combined result of weight loss and shrinkage as a function of firing temperature produces the dramatic temperature dependence of specimen density shown in Fig. 8. A slight increase in density is observed through 1450°C due to normal sintering, but above 1550°C, and consistent with the increasing weight loss shown in Fig. 6, the specimen density decreases. The density decrease becomes more pronounced as G/A increases.

Details of the microstructural development in specimens subjected to the firing schedules discussed in Figs. 6 to 8 are illustrated in the photomicrographs of polished cross sections shown in Fig. 9. A direct comparison can be made in Fig. 9 of the microstructural development in a specimen containing no graphite additive (G/A=0) with that of a specimen having a G/A ratio of 0.75. The pure-alumina specimen exhibits densification by conventional sintering mechanisms, i.e. with increasing temperature, strength develops by neck formation between the particles, followed by pore closure and grain growth. Figure 9 shows that specimens having a G/A of 0.75 follow a progression of microstructural development typical of other levels of graphite additions but entirely different from that of pure alumina. In specimens having a G/A of 0.75, development of two-phase regions is observed after the 1450°C firing (the bright, high-aspect ratio particles are unreacted graphite). The two-phase regions, which become more highly developed during the 1550°C firing, consist of bright particles of alumina nearly surrounded by a light gray matrix of Al_4O_4C (the dark gray is the epoxy mounting medium and the black areas are regions of pullout). The regions between the agglomerates contain coarsened and rounded particles of alumina with no evidence of unreacted graphite. During the 1650°C firing the agglomerates begin to disappear, with the disappearance starting at the surface of the sample and progressing with time toward the center, as was also observed in the "wet" H_2 firings of Fig. 5. The 1650°C microstructure shown in Fig. 9 is taken from the center of a specimen and shows that the alumina particles encapsulated by the aluminum oxycarbide agglomerates have not undergone grain-coarsening, whereas the free alumina particles have coarsened. The microstructure at the surface of the sample fired at 1650°C is similar to that observed throughout the sample fired at 1750°C and exhibits only interconnected, rounded, and coarsened particles of α -alumina, contributing to an extremely low-density specimen.

The rapid nucleation and growth of the intermediate aluminum oxycarbide phase, which involves encapsulation of unreacted alumina particles, establishes that the reaction proceeds through the gas phase. The rapid weight loss associated with disappearance of the oxycarbide suggests that the decomposition proceeds through the loss of volatile products. Both observations are contrary to the conclusion by Cox and Pidgeon⁸ that reactions in the system Al-O-C proceed through the solid state.

Figure 10 shows that the weight loss and microstructural development are highly dependent on the dew point of the firing atmosphere. Figure 10 plots the percent weight loss from samples with a G/A of 0.5, fired for 30 min at 1750°C, as a function of the dew point of the hydrogen atmosphere. The total weight loss diminishes slightly as the dew point is increased up to approximately -5°C. As the dew point is increased beyond -5°C, the percent weight loss drops very rapidly due to retention of the intermediate phase, Al_4O_4C . Metallographic examination of the fired specimens revealed that the pore size at the surface of the specimens becomes increasingly smaller as the dew point of the firing atmosphere increases from -37° to -10°C. At dew points greater than -10°C, the surface layer develops into a fully dense skin of alumina completely encapsulating the specimen.

The path and mechanisms for reaction between alumina and graphite have not been determined, but Figs. 5 and 9 indicate that an intermediate phase, aluminum oxycarbide (Al_4O_4C), forms and disappears with the final production of volatile aluminum suboxides (i.e. AlO , Al_2O) and oxides of carbon. Although Cox and Pidgeon⁸ proposed that the reactions between alumina and carbon are solid-solid, the observations of this investigation indicate that vapor-phase reactions indeed play the dominant role kinetically.

The fact that increasing graphite additions diminish specimen

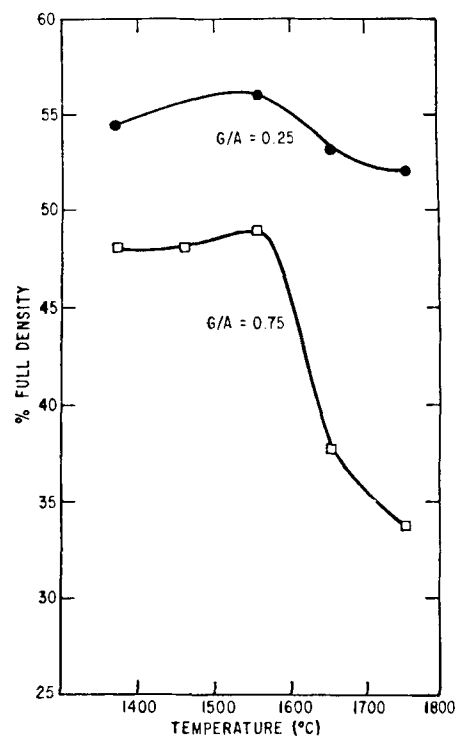


Fig. 8. Temperature dependence of percent theoretical density attained for compacts with G/A molar ratios of 0.25 and 0.75 and fired in "dry" H_2 for 30 min.

density and also firing shrinkage is a manifestation of the existence of aluminum suboxide species. Figure 8 shows that the reaction between alumina and graphite is relatively ineffective in retarding densification of the alumina below 1550°C. The most effective mode of material transport in the system alumina/carbon below 1550°C is apparently either volume or grain-boundary diffusion, both of which contribute to densification. Above 1550°C, an appreciable, direct reaction occurs between graphite and alumina and "evaporation-condensation" becomes the dominant mass-transport mechanism. If the rate of mass transport through the vapor phase is much greater than mass transport by volume or grain-boundary diffusion, coarsening of the grains occurs with a concomitant reduction in surface area and no reduction in pore volume (i.e. no densification).⁹ The flow of hydrogen through the furnace permitted a portion of the volatile suboxides to be swept away and oxidized downstream, resulting in a net weight loss. The open and interconnected porosity associated with rounded particles connected by narrow necks (Fig. 2) is reminiscent of the microstructures of silicon and silicon carbide reported by Greskovich and Rosolowski.¹⁰ They attributed the coarsening of the microstructure to material transport being dominated by evaporation-condensation and surface diffusion rather than by volume or grain-boundary diffusion.

Firings conducted in a "wet" hydrogen atmosphere with a dew point greater than -10°C at 1750°C constitute special cases which result in the formation of a 95%-dense surface layer of α - Al_2O_3 completely surrounding the porous body. It is believed that evolution of CO within the compact serves to maintain a low P_{O_2} and thus stabilize the aluminum suboxides. As the evolved aluminum suboxides and CO effuse toward the surface of the compact, the higher P_{O_2} of the firing atmosphere permits oxidation of the suboxides and concomitant condensation at the surface as α - Al_2O_3 .

IV. Conclusions

(1) Reactions occurring in the system Al-O-C give rise to substantial changes in the densification behavior of alumina and its concomitant microstructure development.

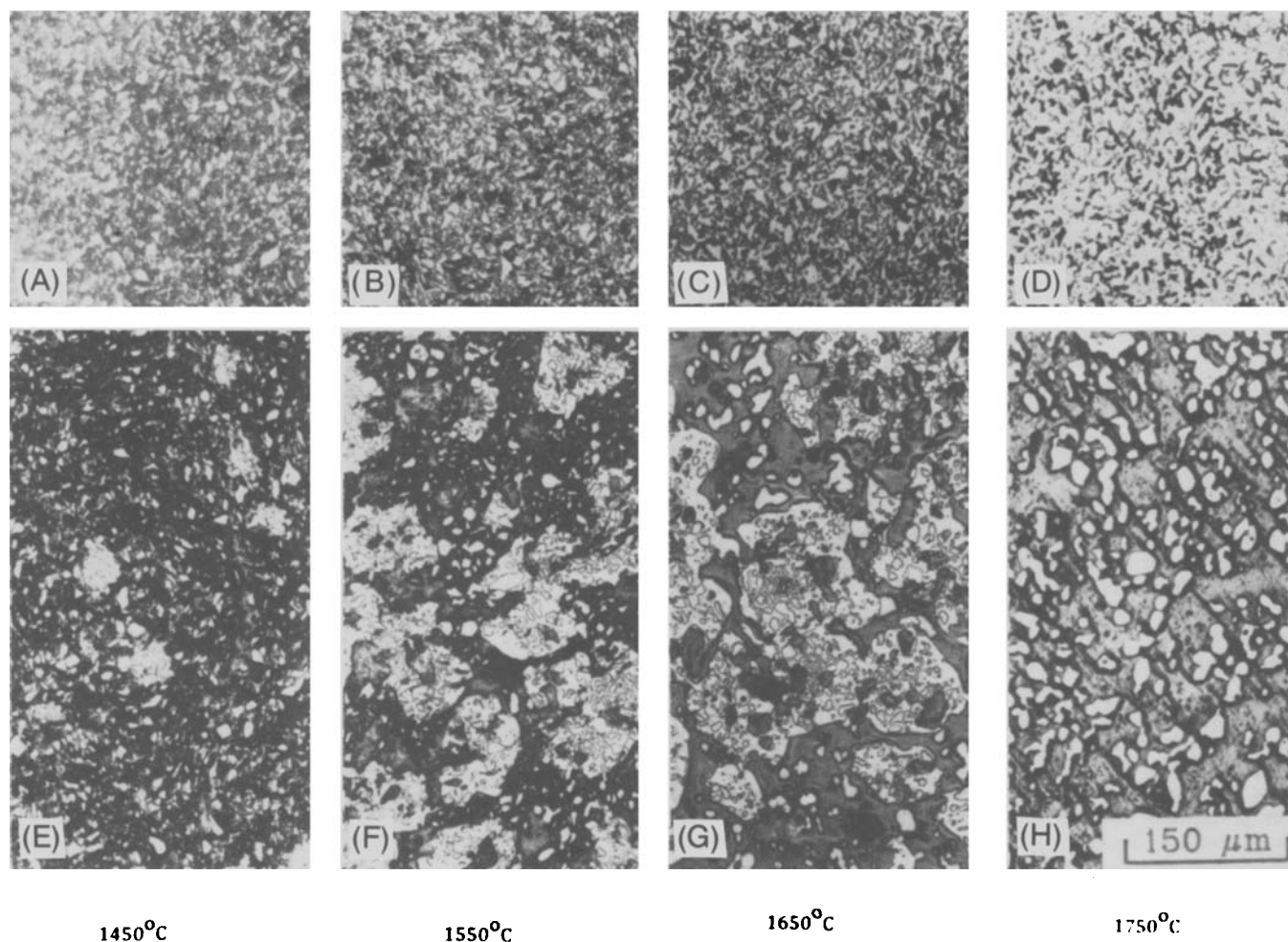


Fig. 9. Microstructural development as a function of temperature for a 30-min isothermal hold under H_2 ($-37^\circ C$ dewpoint). (A) $1450^\circ C$, $G/A=0$; (B) $1550^\circ C$, $G/A=0$; (C) $1650^\circ C$, $G/A=0$; (D) $1750^\circ C$, $G/A=0$; (E) $1450^\circ C$, $G/A=0.75$; (F) $1550^\circ C$, $G/A=0.75$; (G) $1650^\circ C$, $G/A=0.75$; (H) $1750^\circ C$, $G/A=0.75$.

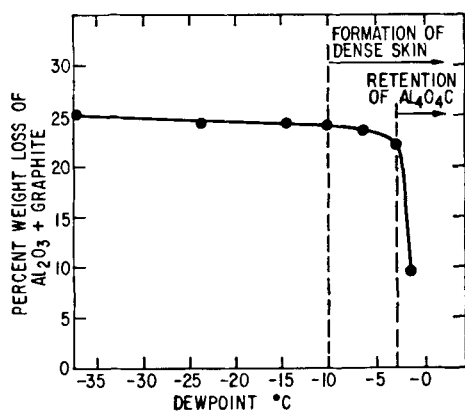


Fig. 10. Plot of percent weight loss of graphite and alumina as a function of firing atmosphere for samples with $G/A=0.5$ fired at $1750^\circ C$ for 30 min, showing dew point range over which a dense alumina skin is formed.

(2) The rate of reaction between graphite and alumina becomes significant above $1550^\circ C$ and proceeds through the intermediate phase, aluminum oxycarbide (Al_4O_4C). The final production of volatile aluminum suboxides contributes to a substantial weight loss.

(3) It is postulated that the presence of volatile aluminum sub-

oxides alters the dominant mass-transport mode from bulk-volume/grain-boundary diffusion to evaporation-condensation.

(4) Proper firing atmosphere control permits the formation of a high-density surface layer of $\alpha-Al_2O_3$ surrounding a highly porous interior.

Acknowledgments: The authors thank S. Prochazka for useful discussions; C. Krystaniak for sintering of samples; J. Methé, J. Grande, and D. Ryan for metallographic sample preparation; D. Marsh for the X-ray analysis; and M. Gill for the scanning electron microscopy.

References

- ¹C. A. Bruch, R. W. Harrison, M. F. X. Gigliotti, M. F. Henry, R. C. Haubert, and C. H. Gay, pp. 258-68 in Proceedings of the Conference on In-Situ Composites, Vol. 3, Ginn Custom Publishing Co., Lexington, MA, 1979.
- ²I. C. Huseby and F. J. Klug, "Chemical Compatibility of Ceramics for Directionally Solidified Ni-Base Eutectic Alloys," *Am. Ceram. Soc. Bull.*, **58** [5] 527-35 (1979).
- ³R. H. Arendt, M. P. Borom, I. C. Huseby, and F. J. Klug, "Molten Salt Leach for Removal of Inorganic Cores From Directionally Solidified Eutectic Alloy Structures," U.S. Pat. 4 082 566, April 4, 1978.
- ⁴M. P. Borom, R. H. Arendt, and N. C. Cook, "Dissolution of Oxides of Y, Al, Mg, and La by Molten Fluorides," *Am. Ceram. Soc. Bull.*, **60** [11] 1168-74 (1981).
- ⁵M. P. Borom, "Dissolution of Single and Mixed Oxides of Y, La, Al, Mg in Aqueous Caustic," *Am. Ceram. Soc. Bull.*, **61** [2] 221-26, 230 (1982).
- ⁶P. D. S. St. Pierre and M. J. Curran, "A Simple Laboratory Furnace for Use to $2500^\circ C$," GETIS Rept. No. 72CRD012, 1971.
- ⁷F. J. Klug, W. D. Pasco, and M. P. Borom, "Relationship Between Microstructure and Crushability of Porous Ceramic Bodies," unpublished work.
- ⁸J. H. Cox and L. M. Pidgeon, "An Investigation of the Aluminum-Oxygen-Carbon System," *Can. J. Chem.*, **41**, 671-83 (1963).
- ⁹R. L. Coble and R. M. Cannon, "Current Paradigms in Powder Processing"; in Processing of Crystalline Ceramics, Edited by H. Palmour III, R. F. Davis, and T. M. Hare, Plenum, New York, 1978.
- ¹⁰C. Greskovich and J. H. Rosolowski, "Sintering of Covalent Solids," *J. Am. Ceram. Soc.*, **59** [7-8] 336-43 (1976).